Biol. Chem., Vol. 391, pp. 219–227, February/March 2010 • Copyright © by Walter de Gruyter • Berlin • New York. DOI 10.1515/BC.2010.015

The epimerase activity of anthocyanidin reductase from *Vitis vinifera* and its regiospecific hydride transfers

Mahmoud Gargouri[1,2], Jean Chaudière[1,*], Claude Manigand[1], Chloé Maugé[1], Katell Bathany[1], Jean-Marie Schmitter[1] and Bernard Gallois[1]

[1] Chimie et Biologie des Membranes et des Nanoobjets UMR CNRS 5248, Bâtiment B8, Avenue des Facultés, Université Bordeaux 1, F-33405 Talence Cedex, France
[2] Laboratoire de Physiologie Moléculaire des Plantes, Centre de Biotechnologie de Borj-Cedria, B.P. 901, 2050 Hamman-Lif, Tunisia

*Corresponding author
e-mail: j.chaudiere@cbmn.u-bordeaux.fr

Abstract

Anthocyanidin reductase (ANR) from *Vitis vinifera* catalyzes an NADPH-dependent double reduction of anthocyanidins producing a mixture of (2S,3R)- and (2S,3S)-flavan-3-ols. At pH 7.5 and 30°C, the first hydride transfer to anthocyanidin is irreversible, and no intermediate is released during catalysis. ANR reverse activity was assessed in the presence of excess $NADP^+$. Analysis of products by reverse phase and chiral phase HPLC demonstrates that ANR acts as a flavan-3-ol C_3-epimerase under such conditions, but this is only observed with 2R-flavan-3-ols, not with 2S-flavan-3-ols produced by the enzyme in the forward reaction. In the presence of deuterated coenzyme 4S-NADPD, ANR transforms anthocyanidins into dideuterated flavan-3-ols. The regiospecificity of deuterium incorporation into catechin and afzelechin – derived from cyanidin and pelargonidin, respectively – was analyzed by liquid chromatography coupled with electrospray ionization-tandem mass spectrometry (LC/ESI-MS/MS), and it was found that deuterium was always incorporated at C_2 and C_4. We conclude that C_3-epimerization should be achieved by tautomerization between the two hydride transfers and that this produces a quinone methide intermediate which serves as C_4 target of the second hydride transfer, thereby avoiding any stereospecific modification of carbon 3. The inversion of C_2 stereochemistry required for 'reverse epimerization' suggests that the 2S configuration induces an irreversible product dissociation.

Keywords: anthocyanidin reductase; deuterium labeling; double reduction; epimerase; hydride transfer; NADPH; quinone methide; regiospecificity.

Introduction

For the past decade, the expression and partial characterization of several enzymes (see Scheme 1) have greatly improved our understanding of the biosynthetic pathway(s) of flavan-3-ols of distinct stereochemistries from leucoanthocyanidins produced by dihydroflavonol reductase (DFR). In the first pathway, a reductive dehydration step performed by leucoanthocyanidin reductase (LAR) converts leucoanthocyanidins to (2R,3S)-*trans*-flavan-3-ols such as (+)-catechin (Tanner et al., 2003; Pfeiffer et al., 2006). In parallel, anthocyanidin synthase (a dioxygenase) transforms leucoanthocyanidins into chromophoric anthocyanidins (Saito et al., 1999; Turnbull et al., 2001; Wilmouth et al., 2002; Abrahams et al., 2003). The latter are unstable compounds which could be either glycosylated by UDP-glucose:flavonoid 3-O-glucosyltransferase into anthocyanins (Springob et al., 2003; Veitch and Grayer, 2008) or reduced by anthocyanidin reductase (ANR, EC 1.3.1.77) into flavan-3-ols at the expense of two NADPH equivalents (Xie et al., 2003).

There are very few enzymes that use two equivalents of a nicotinamide coenzyme to reduce a single cosubstrate. In addition to ANR, the best documented examples are probably the NADPH-dependent pteridine reductase PTR1 from *Leishmania tarentolae* and *Leishmania major* (Wang et al., 1997; Gourley et al., 2001), and the recently described NAD(P)H-dependent diketoreductase from *Acinetobacter baylyi* (Wu et al., 2009). A mechanistic study of the regio- and stereospecificity of ANRs would therefore help to understand the unusual potentialities of this enzyme family. In a comparative study of ANR from *Arabidopsis thaliana* and *Medicago truncatula* (*At*- and *Mt*-ANR in Scheme 1), Xie et al. (2004) reported that (-)-epicatechin [(2R,3R) *cis* structure] was the major reduction product of cyanidin in either case, and they assumed that the minor amount of (-)-catechin [(2S,3R) *trans* structure] which was additionally produced might be as a result of non-enzymatic epimerization. They proposed a speculative but plausible reductive mechanism in which two hydride transfers from NADPH to carbons 2 and 3 of cyanidin would lead to a 2,3-*cis* product of unique stereochemistry, i.e., (2R,3R). However, in a recent report (Gargouri et al., 2009a), we showed that ANR from *Vitis vinifera* (*Vv*-ANR) exclusively used pro(S) hydrogen from NADPH and we provided non-equivocal evidence for the enzyme-mediated production of a mixture of C_3-epimers of 2S configuration, such as (-)-catechin and (+)-epicatechin derived from cyanidin. Thus, *Vv*-ANR does not only behave as a reductase but also as a C_3-epimerase, which suggests that its

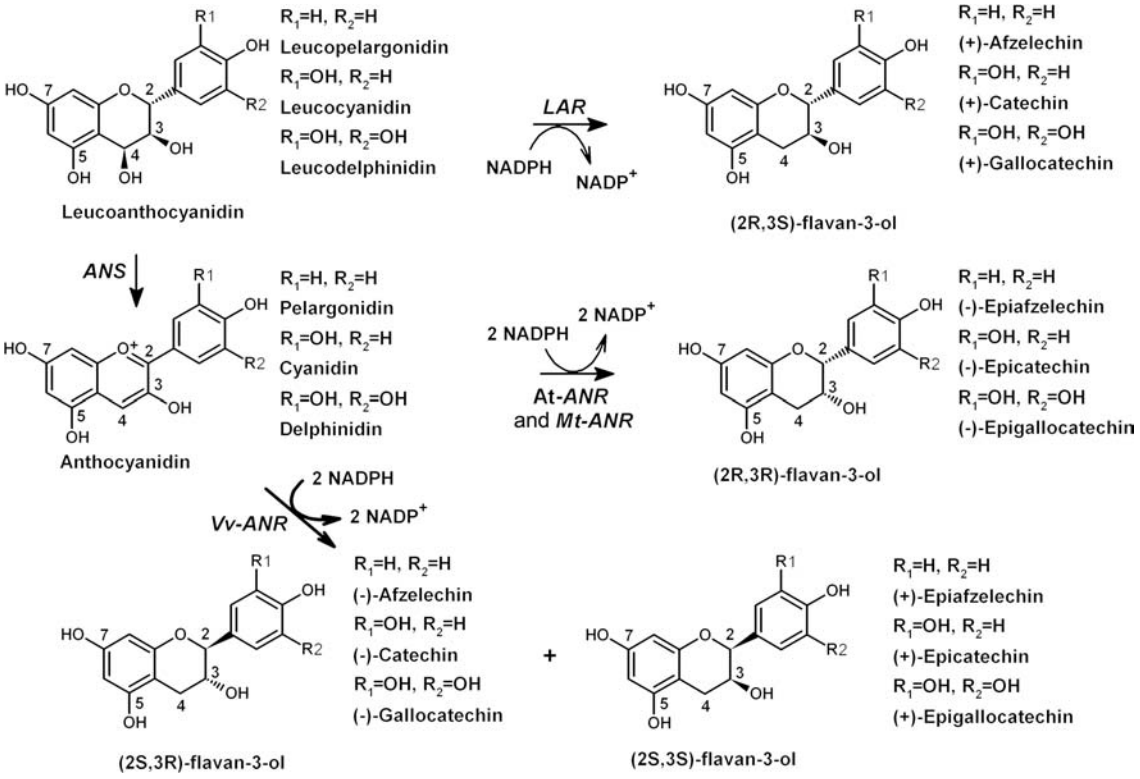

Scheme 1 Biosynthetic pathways of flavan-3-ols.

catalytic mechanism could substantially differ from that of previously described ANRs. Our subsequent studies of steady-state kinetics and binding at equilibrium (Gargouri et al., 2009b) led to the conclusion that the kinetic mechanism of *Vv*-ANR was rapid-equilibrium ordered (Bi Uni Uni Bi), with NADPH binding first and $NADP^+$ released last. In the present study, we investigated the regiospecificity of hydride transfers to anthocyanidins by means of deuterium-labeling and LC/ESI-MS/MS experiments, and we demonstrated that the enzyme performs as a pure C_3-epimerase of 2R-flavan-3-ols in the presence of excess $NADP^+$. Our results provide mechanistic clues to the epimerase activity which is associated with anthocyanidin reduction or flavan-3-ol oxidation.

Results

Cyanidin strongly absorbs visible light with a maximal absorbance wavelength of 578 nm ($\varepsilon \sim 16\ 533\ M^{-1}\ cm^{-1}$) at pH 7.5, and this wavelength was used to monitor the time course of cyanidin disappearance with or without ANR. Methanolic samples of products derived from either cyanidin or pelargonidin upon completion of the ANR-mediated reaction were resolved by reverse phase and chiral phase HPLC. As shown in the reverse phase chromatogram of Figure 1A, cyanidin is transformed into equivalent amounts of flavan-3-ols having the retention times of catechin (peak 1) and epicatechin (peak 2). Based on the chiral phase chromatogram shown in Figure 1B, we confirm (Gargouri et al., 2009a) that these two flavan-3-ols are (-)-catechin and (+)-epicatechin.

To assess the possibility that ANR exhibits significant catalytic activity in the backward direction of the reaction, the enzyme was then incubated at pH 7.5 and 30°C with each of the four (epi)catechin stereoisomers in the presence of a large concentration of $NADP^+$. No trace of 578-nm chromophore could be detected in any of these four experiments. Moreover, (-)-catechin and (+)-epicatechin were both recovered unchanged from the reaction medium, even upon 16 h of incubation in the presence of 50 μM ANR.

However, as shown in Figure 2, we found that (+)-catechin and (-)-epicatechin were independently transformed into their C_3-epimer. In either case, the yield of epimerization exceeded 30% upon a 30-min incubation of 50 μM flavanol with 50 μM ANR and 500 μM $NADP^+$. There was no spontaneous isomerization in the absence of ANR, and with only 5 μM ANR the yield of epimerization was approximately twice smaller by 30 min.

It was also approximately twice smaller by 16 h when the reaction medium contained 100 μM NADPH in addition to 500 μM $NADP^+$. Thus, ANR has the unexpected property to slowly but selectively epimerize 2R epimers of its own reduction products when the ratio $[NADP^+]/[NADPH]$ is high. This 'reverse' C_3-epimerase activity is not associated with irreversible consumption of $NADP^+$, for there is no measurable increase in 340-nm absorbance.

The regiospecificity of hydride transfers from NADPH to either cyanidin (phenolic ring B) or pelargonidin (catecholic

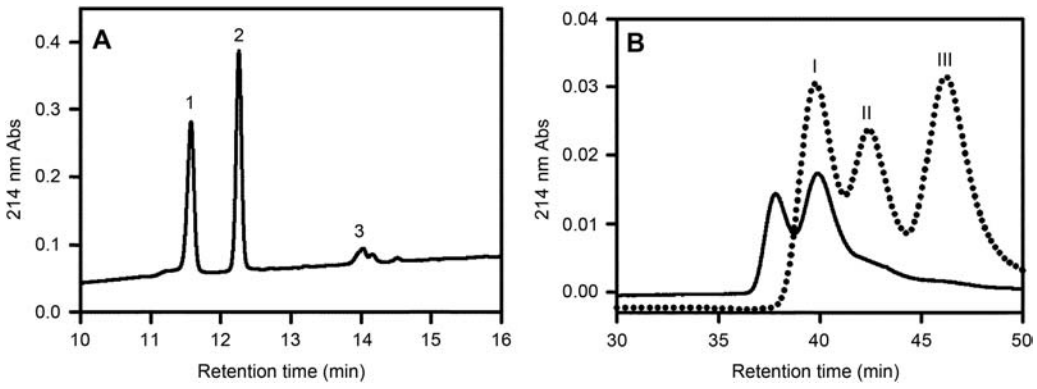

Figure 1 Chromatographic analysis of products derived from cyanidin in the presence of ANR and excess NADPH.
Initial concentrations are 200 μM NADPH and 50 μM cyanidin. (A) Reverse-phase HPLC; peak 1 is eluted at the retention time of the two catechin standards, whereas peak 2 is eluted at the retention time of the single epicatechin standard; peak 3 contains a dimer of cyanidin. (B) Chiral phase HPLC; external standards indicated by the dotted line: (-)-catechin [I], (-)-epicatechin [II], and (+)-catechin [III].

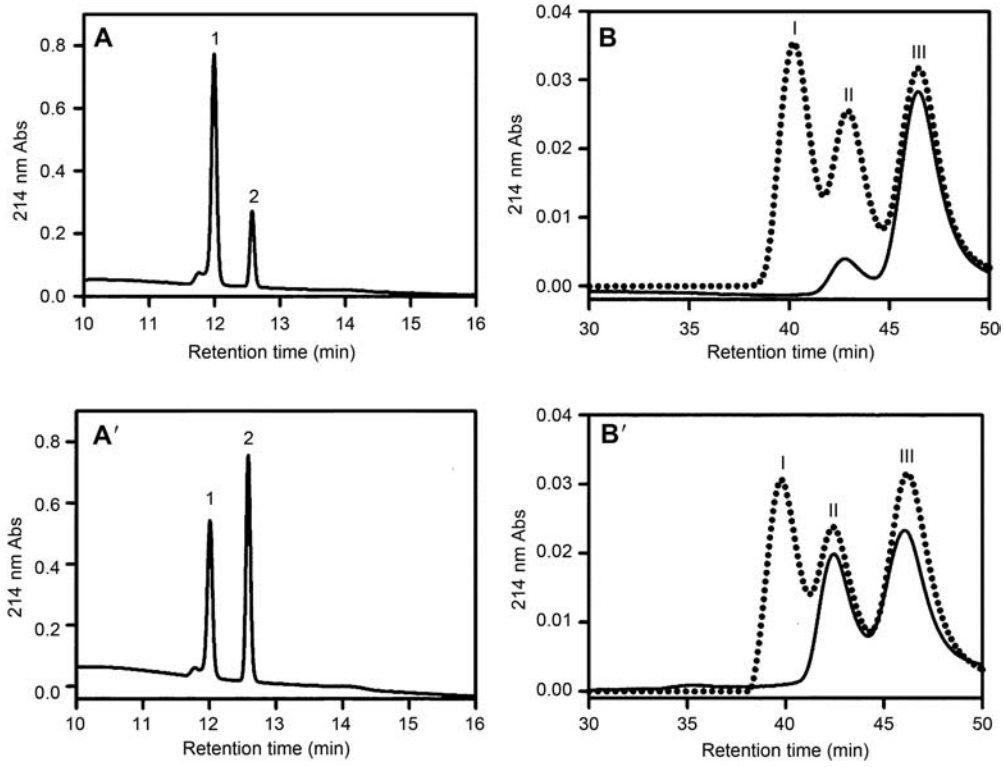

Figure 2 Chromatographic analysis of products derived from 2R-flavan-3-ols in the presence of ANR and excess $NADP^+$.
(A, A′) Reverse phase HPLC; peaks 1 and 2 contain catechins and epicatechins, respectively, as in Figure 1. (B, B′) Chiral phase HPLC. Samples are methanolic solutions of polyphenols obtained upon 30-min incubation of 50 μM ANR with 500 μM $NADP^+$ and 50 μM flavan-3-ol at pH 7.5 and 30°C; flavan-3-ols initially introduced are (+)-catechin in (A) and (B), and (-)-epicatechin in (A′) and (B′); external standards shown by the dotted line: (-)-catechin [I], (-)-epicatechin [II], and (+)-catechin [III].

ring B) was then investigated by means of deuterium labeling. For this purpose, 4S-NADPD was substituted for NADPH, and the deuterated products were analyzed by LC-MS and LC-MS/MS. Positive ion mass spectra of enzymatically deuterated catechin and afzelechin are reproduced in Figures 3 and 4, respectively. In Figure 3A, the major ion at *m/z* 293 can be assigned to an ($M+H^+$) ion derived from dideuterated catechin, in agreement with the expected double reduction of cyanidin. The relative abundance of the peak at *m/z* 294 is in agreement with the expected value for catechin (isotopic contribution of ^{13}C). Similar conclusions can be drawn from Figure 4A: the spectrum attributed to dideuterated afzelechin is virtually the same if one takes into account the expected 16-Da shift in *m/z* values.

MS/MS spectra of precursor ions at *m/z* 293 and 277 are shown in Figures 3B and 4B, respectively. For dideuterated catechin (Figure 3B), major fragments have *m/z* values of 124, 140, and 167. The corresponding fragments occur at *m/z* 108, 140, and 151 in the MS/MS spectrum of dideuterated afzelechin (Figure 4B). Our interpretation of the MS/MS spectra of dideuterated catechin and afzelechin is summarized in Tables 1 and 2 (peaks assigned to ^{13}C background result from the isolation width of the precursor ion that was isolated with its isotopic cluster). This interpretation is based on the *m/z* values of MS/MS fragments which we observed with non-deuterated catechin and afzelechin. All such values are reported in Scheme 2 which confirms most

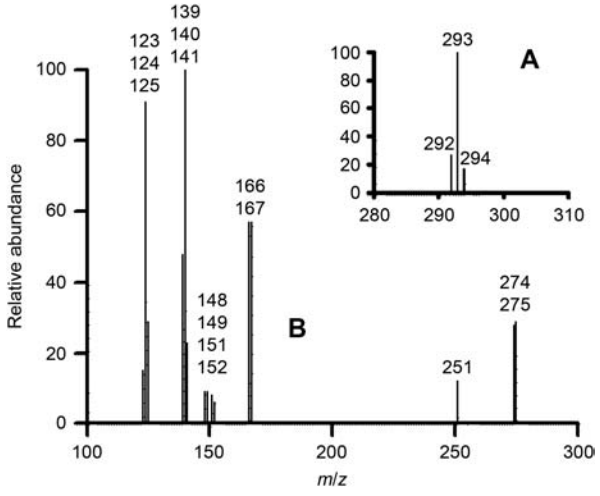

Figure 3 Positive ion mass spectra of enzymatically deuterated catechin.
(A) ESI-MS spectrum; (B) MS/MS spectrum of the major ESI-MS ion (*m/z* 293).

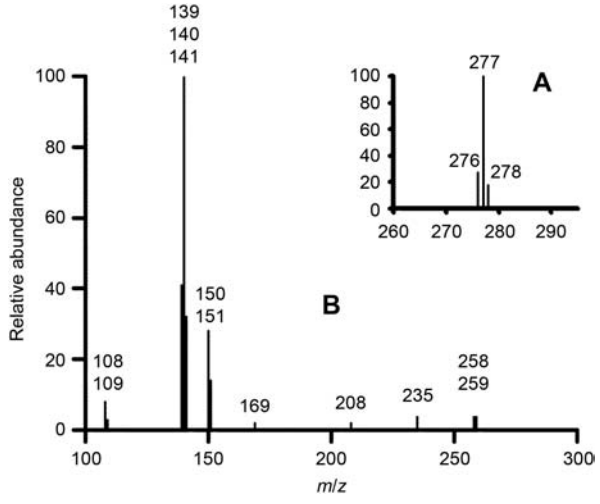

Figure 4 Positive ion mass spectra of enzymatically deuterated afzelechin.
(A) ESI-MS spectrum; (B) MS/MS spectrum of the major ESI-MS ion (*m/z* 277).

of the fragmentation steps reported by Li and Deinzer (2007) for catechin (*m/z* values outside parentheses) and uses our own data to extend them to afzelechin (*m/z* values inside parentheses). Clearly, the conclusion which can be drawn from Tables 1 and 2 is that the two deuterium transfers have been targeted to C_2 and C_4, respectively. The lack of *m/z* 170 monodeuterated fragment in the MS/MS spectrum of catechin is not surprising, because the abundance of the corresponding (*m/z* 169) fragment reported by Li and Deinzer (2007) for non-deuterated catechin was extremely low and actually undetectable in our own spectra (see Scheme 2). The abundance of the *m/z* 149 fragment is low but significant in the MS/MS spectrum of deuterated catechin, and the absence of the corresponding fragment (*m/z* 133) in that of deuterated afzelechin is likely to reflect the influence of changing phenol for catechol in ring B. Finally, the *m/z* 251 fragment ion of deuterated catechin does not have a corresponding *m/z* 249 or 250 fragment in the MS/MS spectrum of non-deuterated catechin reported by Li and Deinzer (2007), as well as in our own data (see Scheme 2). A similar fragmentation is observed for deuterated afzelechin with a 16-Da mass shift, leading to the *m/z* 235 ion. Although it is tempting to think that it results from a loss of ethynol (loss of 42 Da), we cannot use it in an analysis of deuteration regiospecificity because we do not have a realistic fragmentation pathway to suggest.

Discussion

The two hydrides which are sequentially transferred to anthocyanidin come from pro(S) hydrogens of NADPH, and the three-dimensional structure of the apoenzyme exhibits a single Rossman fold. Moreover, binding equilibrium data support a single NADPH-binding site per enzyme molecule (Gargouri et al., 2009a,b). This means that the orientation of these two transfers should be the same, either from above or from below the average plane of the benzopyran ring. Our data suggest that the first reduction step is virtually irreversible because no trace of anthocyanidin could be observed at the 578 nm wavelength in the backward reaction, even with 2R-flavanols for which the last step is apparently reversible. Because no significant amount of polyphenolic structures other than anthocyanidin and two flavan-3-ol epimers could be visualized in any of our chromatograms, it is likely that the expected dihydrocyanidin intermediate is tightly bound to the enzyme and never released in the aqueous solvent, and this is in agreement with the rapid-equilibrium ordered mechanism deduced from steady-state kinetics and equilibrium-binding studies (Gargouri et al., 2009b). The second hydride transfer is irreversible with natural products of 2S configuration. However, we did observe C_3-epimerization of 2R-catechin or -epicatechin in the presence of a large excess of $NADP^+$, which means that hydride transfer to 2R-dihydrocyanidin(s) is reversible, but markedly displaced in the direction of $NADP^+$ production. Altogether, these observations suggest that an ANR-dihydrocyanidin transient complex undergoes reversible epimerization between the two steps of

Table 1 Carbon targets of deuterium labeling in the major MS/MS fragments of dideuterated catechin.

m/z[a]	Equivalence[b]	Deuteration	Deuterium position(s)
123	123	Non-deuterated	–
124	123+1	Monodeuterated	**C_2**
125	123+2	Dideuterated	C_{13} background
139	139	Non-deuterated	–
140	139+1	Monodeuterated	**C_4**
141	139+2	Dideuterated	C_{13} background
148	147+1	Monodeuterated	C_2 or C_3 or C_4
149	147+2	Dideuterated	(C_2, C_4) or (C_2, C_3) or (C_3, C_4)
151	151	Non-deuterated	–
152	151+1	Monodeuterated	C_{13} background
166	165+1	Monodeuterated	C_2 or C_3 or C_4
167	165+2	Dideuterated	(C_2, C_4) or (C_2, C_3) or (C_3, C_4)
251	?	?	?
274	273+1	Monodeuterated	C_2 or C_3 or C_4
275	273+2	Dideuterated	(C_2, C_4) or (C_2, C_3) or (C_3, C_4)

[a]*m/z* values of the most abundant fragments are shown in bold font.
[b]*m/z* reference values are those of MS/MS fragments of non-deuterated catechin.

Table 2 Carbon targets of deuterium labeling in the major MS/MS fragments of dideuterated afzelechin.

m/z[a]	Equivalence[b]	Deuteration	Deuterium position(s)
108	107+1	Monodeuterated	**C_2**
109	107+2	Dideuterated	C_{13} background
139	139	Non-deuterated	–
140	139+1	Monodeuterated	**C_4**
141	139+2	Dideuterated	C_{13} background
150	149+1	Monodeuterated	C_2 or C_3 or C_4
151	149+2	Dideuterated[c]	(C_2, C_4) or (C_2, C_3) or (C_3, C_4)
169	169	Non-deuterated	–
208	?	?	?
235	?	?	?
258	257+1	Monodeuterated	C_2 or C_3 or C_4
259	257+2	Dideuterated	(C_2, C_4) or (C_2, C_3) or (C_3, C_4)

[a]*m/z* values of the most abundant fragments are shown in bold font.
[b]*m/z* reference values are those of MS/MS fragments of non-deuterated afzelechin.
[c]Plus non-deuterated *m/z* 151.

hydride transfer. Although we do not know which of the anthocyanidin flavylium cation or quinoidal conjugate bases preferentially binds to ANR as a true substrate, in all cases, the electrophilic target of the first hydride transfer should be either carbon 2 or carbon 4, i.e., those which are in *ortho* or *para* position with regard to oxygen 1.

In the most plausible double-reduction mechanisms that could be envisaged, the second hydride transfer would be targeted to carbon 3, i.e., to a ketone group resulting from tautomerization of either a 4,3- or a 2,3-enol intermediate. These two mechanisms are formally excluded by the deuterium incorporation experiments, because they cannot lead to the observed (C_2, C_4) dideuteration. Moreover, they are incompatible with the observed C_3-epimerization as well as with the production of a mixture of *cis*- and *trans*-products of strict 2S configuration. This means that we have to look for a mechanism in which the observed epimerization at C_3 is actually as a result of non-stereospecific proton addition. Scheme 3 is compatible with such constraints, as well as with the rapid-equilibrium ordered Bi Uni Uni Bi mechanism. In the first step of Scheme 3, a stereospecific reduction at C_2 leads to the enolic structure II which instead of being transformed into its 3-keto equivalent by spontaneous tautomerization undergoes an enzyme-catalyzed tautomerization which leads to quinone methide epimers (structures III and IV). The 2,3-stereochemistry of the final products is already in place at this stage, and the quinone methide structure then provides a good target for a second hydride transfer, this time at C_4. The formation of the two quinone methide epimers requires at least a basic catalytic side chain on the enzyme to facilitate deprotonation of one of the phenolic hydroxyl groups at C_5 or C_7. In principle, the overall proton exchange

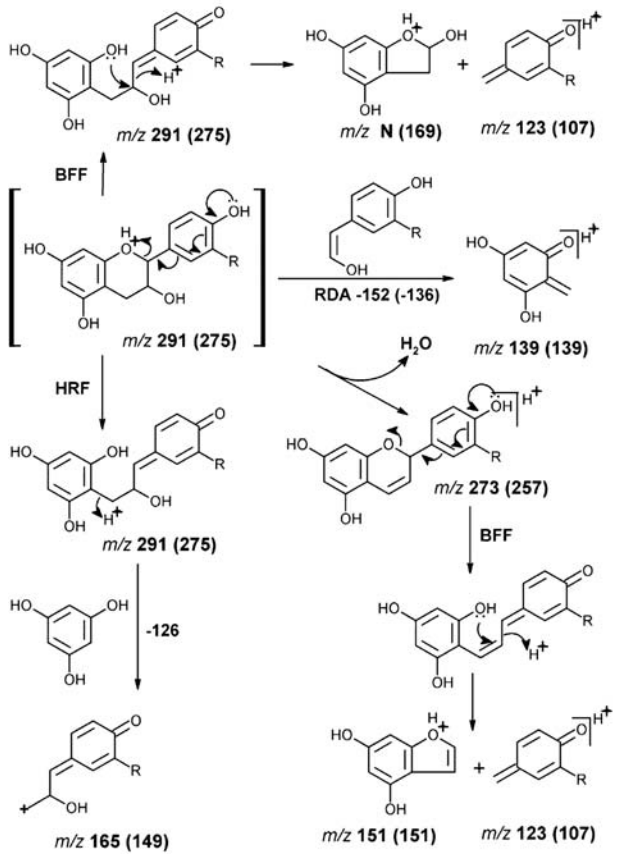

Scheme 2 Fragmentation pathways of catechin[a] and afzelechin[b]. [a](R=OH, *m/z* outside parentheses); [b](R=H, *m/z* inside parentheses); N=not observed.
RDA, Retro Diels-Alder; BFF, benzofuran-forming fission.

would be facilitated by simultaneous acidic catalysis in the vicinity of carbon 3, but a single acidic side chain would favor stereospecific protonation at C_3 instead of the observed epimerization. Therefore, one has to assume that the proton captured by carbon 3 comes from the aqueous solvent.

The involvement of a quinone methide intermediate as a target of the second hydride transfer is the most plausible explanation of deuteration at C_4. Moreover, this structure bears striking resemblance with the quinone methide intermediate which is the target of hydride transfer in eugenol synthase, an NADPH-dependent reductase (Louie et al., 2007). Interestingly, recent structural data obtained in our laboratory strongly support the involvement of a similar quinone methide intermediate in the catalytic mechanism of LAR (Maugé et al., in preparation). In LAR, the production of a quinone methide should result from a dehydration step. With ANR, none of the structures that could be envisaged as a partial reduction intermediate of anthocyanidin would enable such a dehydration mechanism, and this is why Scheme 3 assumes that it results from proton exchange between the phenolic hydroxyl at C_5 or C_7 and the enolic carbon 3 of structure II.

If Scheme 3 is essentially correct, it should be compatible with the reverse epimerase activity of ANR, even if the latter

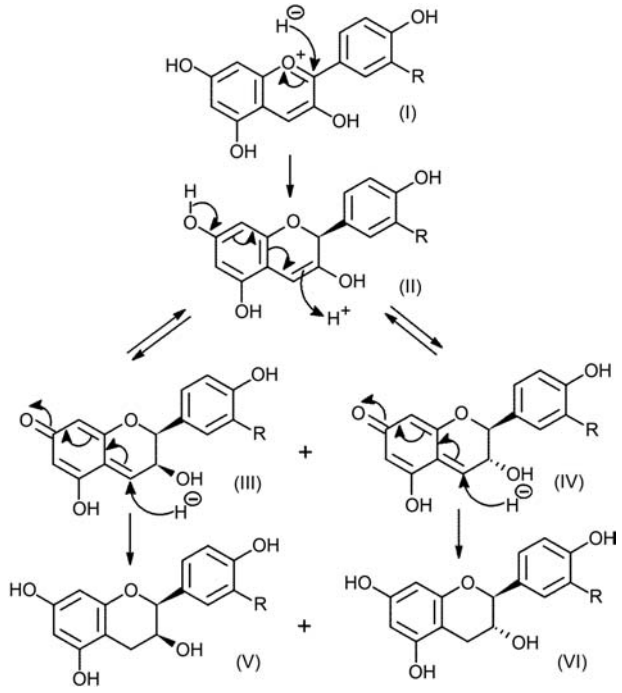

Scheme 3 (C_2, C_4) sequence of hydride transfers in the forward reaction.

is only observed with 2R-flavan-3-ols which are C_2-epimers of its 'normal' products in the forward reaction. This activity requires $NADP^+$, which suggests that hydride transfer from flavan-3-ol to $NADP^+$ is the first step (Scheme 4). For such a dehydrogenation step, proton extrusion is an absolute prerequisite of hydride delivery, and this leaves CH in positions 2, 3, and 4 as possible sources of hydride. In the forward pathway, hydride delivery from NADPH to carbon 2 produces a 2S structure, which means that CH in position 2 of

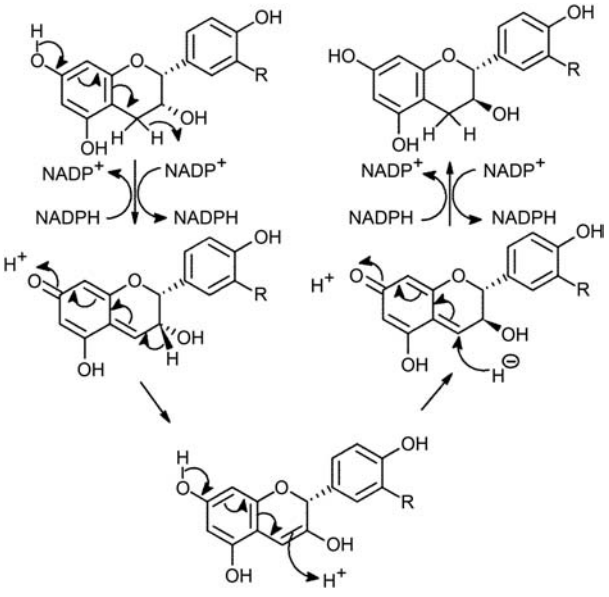

Scheme 4 Reverse epimerization.

2R-flavanols could not deliver a hydride ion to $NADP^+$ in the reverse pathway, following deprotonation of a phenolic or aliphatic hydroxyl. Moreover, the epimerization that is observed at C_3 is just as efficient with flavan-3-ols of (2R,3R) configuration as with flavan-3-ols of (2R,3S) configuration. This means that we can rule out hydrogenated carbon 3 as a source of hydride, because the oxidized nicotinamide ring of $NADP^+$ must stack on its polyphenolic partner in the same configuration as the reduced nicotinamide ring of NADPH in the forward pathway, hydride transfer from carbon 3 of (+)-catechin to $NADP^+$ can be ruled out, and we conclude that the hydride ion transferred to $NADP^+$ should come from the methylene group in position 4, which strongly supports a (C_2, C_4) sequence of hydride transfers in the forward/reductive pathway. In other words, our 'reverse epimerization' data support the reductive (C_2, C_4) sequence of Scheme 3, but not a (C_4, C_2) sequence.

The reverse epimerization pathway would then be described by Scheme 4, which might not require any other catalytic assistance than that which was assumed for Scheme 3. In the presence of a large excess of $NADP^+$, the ANR/$NADP^+$/flavan-3-ol complex would be in equilibrium with an ANR·NADPH·quinone methide complex, and the latter would slowly epimerize through interconversion with its enolic tautomer. The fact that this reverse epimerization only works with 2R-flavan-3-ols is more puzzling. This could be as a result of a much higher dissociation constant of 2S-flavan-3-ols from the last ternary complex. A 2S-induced geometrical constraint would indeed solve the problem of product release, which is frequently the limiting step in NAD(P)(H)-dependent enzymes.

A critical feature of Scheme 3 is the C_4-regiospecificity of the second hydride transfer, i.e., that which is also observed with the closest structural homologs of ANR. A search for potential structural homologs led to the conclusion that the enzyme that has the greatest three-dimensional homology with ANR is DFR from *Vitis vinifera*, another enzyme of the short-chain dehydrogenase/reductase superfamily which is known to transfer a hydride equivalent to carbon 4 of dihydroflavonols (Petit et al., 2007). The root mean square distance obtained by alignment of the two matrices was 1.6 Å, with 253 aligned Cα positions. The structural homolog that ranked second to DFR in this search was vestitone reductase, an NADPH-dependent enzyme which reduces 2-hydroxy-isoflavanone-3R vestitone, here again by means of hydride transfer to carbon 4 of the benzopyran ring (Shao et al., 2007). As already mentioned, an enzyme-assisted deprotonation of a phenolic hydroxyl group at C_5 or C_7 is necessary to produce quinone methide intermediates of Scheme 3. The catalytic triad of the short-chain dehydrogenase/reductase superfamily includes a lysine and a tyrosine residue which could fulfill this function, and which are conserved in ANR (Tyr_{168} and Lys_{172}) and DFR (Tyr_{163} and Lys_{167}) from *Vitis vinifera*. In DFR, the side chain of Tyr_{163} is indeed at hydrogen-bonding distance from the C_5 hydroxyl group (Petit et al., 2007). With ANR, a three-dimensional structural assessment of our mechanistic predictions is not possible at this time, because all attempts to crystallize a binary or ternary complex of ANR have been unsuccessful. In the three-dimensional structure of the crystallized apoenzyme (Gargouri et al., 2009a), the active site is virtually locked in a configuration that would hardly leave any space for binding of either NADPH or cyanidin, because it is obstructed by a large peptidic loop.

In conclusion, we have shown that *Vv*-ANR performs as a pro(S) reductase/C_3-epimerase in the forward direction of the reaction with hydride transfers at C_2 and C_4, whereas it performs as a pure C_3-epimerase in the backward direction. The 'reverse' epimerase activity requires the presence of ANR and $NADP^+$, and instead of being observed with the products of the forward reaction it is exclusively observed with the corresponding C_2-epimers. The most plausible mechanism that could be envisaged from our data relies on the transient production of an enzyme-bound quinone methide intermediate following a first hydride transfer at C_2, and it implies a strict C_4-regiospecificity of the second hydride transfer. The (C_2, C_4) regiospecificity of the two hydride transfers would therefore provide a mechanistic rationale for C_3-epimerization in the forward and backward directions of the reaction.

Materials and methods

Chemicals, enzymes and reagents

Cyanidin chloride, pelargonidin chloride, (+)-catechin, and (-)-epicatechin were purchased from Extrasynthèse (Genay, France). (-)-Catechin ≥98% pure, glucose-6-phosphate dehydrogenase from Baker's yeast type XV, dithiothreitol, NADPH tetrasodium salt ≥97% pure, $NADP^+$ sodium salt, D-Glucose-1-d, antibiotics, and all buffer components were purchased from Sigma-Aldrich Chemical Co. (S)-NADPD, i.e., 4S-$NADP^2H$, was synthesized enzymatically, as previously described (Gargouri et al., 2009a).

Expression and purification of recombinant *Vv*-ANR

A cDNA library isolated from *Vitis vinifera* Cabernet Sauvignon post-veraison berries was used for PCR amplification of the open reading frame of the *Vv-ANR* gene. All steps, including PCR amplification, production of a His_6-tag fused GB1-ANR construct, expression of His_6-tagged fused protein GB1-ANR in *Escherichia coli*, Tev-mediated removal of the GB1 domain including the hexahistidine tag at its N-terminal end, and purification of *Vv*-ANR to homogeneity, were performed as previously described (Gargouri et al., 2009a). *Vv*-ANR was concentrated by ultrafiltration and stored at -20°C upon dialysis against 10 mM tricine, 50 mM NaCl, 10 mM dithiothreitol, 5 mM EDTA, pH 7.5, plus 2.5% glycerol (v/v). ANR protein concentration was measured by monitoring the absorbance at 280 nm, using a theoretical extinction coefficient of 28 795 M^{-1} cm^{-1}.

Enzyme assays

Anthocyanidin reductase assays were carried out at pH 7.5 and 30°C in the forward and backward directions of the reaction. Two distinct incubation times (30 min and 16 h) were used for each assay. Reaction products were then extracted with 2×500 µl ethylacetate, supernatants were pooled and dried under argon and the products were dissolved in 40 µl methanol, stored at -20°C or directly used

for HPLC analysis. In the forward direction, the enzyme activity was assayed in a buffer containing 50 mM HEPES, pH 7.5, plus 5% methanol (v/v), 50 μM anthocyanidin chloride, 200 μM NADPH, and 2 μM enzyme in a total volume of 200 μl. Anthocyanidins were always introduced last in final reactional media as aliquots of stock solutions prepared in methanol containing 4% (v/v) of methane sulfonate buffer (10 mM, pH 2), and diluted to the appropriate concentrations by monitoring the maximal absorbance in the visible region. The spontaneous degradation of such stock solutions was undetectable for 24 h at 4°C, and for at least 4 days at -20°C. In the backward direction, the enzyme activity was assayed in a buffer containing 50 mM HEPES, pH 7.5, plus 5% methanol, 50 μM *cis*- or *trans*-flavan-3-ol of defined stereochemistry, 500 μM $NADP^+$ and 5 or 50 μM enzyme in a total volume of 200 μl. For the experiment which required (+)-epicatechin, the latter was first prepared from the forward (reducing) reactional medium, using a semi-preparative dc18 reverse phase column of 10-mm diameter and the same elution system as that described below with the analytical column.

Routine HPLC assay of 2,3-*cis*- and 2,3-*trans*-flavan-3-ols produced by ANR

2,3-*cis*-Flavan-3-ols and 2,3-*trans*-flavan-3-ols were routinely resolved and quantified without stereospecific discrimination of the corresponding diastereoisomers. This was achieved with a reverse phase column (Atlantis dc18, 4.6×250 mm, 300 Å, 5 μm, from Waters, Versailles, France) under a flow rate of 1 ml min^{-1}. A linear elution gradient was applied for 20 min, from 10% to 90% acetonitrile, in the presence of 0.08% trifluoroacetic acid. The absorbance wavelength of the detector (996 photodiode Array Detector, Waters) was set at 214 nm to ensure optimal sensitivity. 2,3-*cis*- and 2,3-*trans*-Flavan-3-ols were quantified by means of external standards.

HPLC assay used for stereochemical characterization of (epi)catechin products

Mixtures of polyphenols produced by ANR were extracted and redissolved in methanol as described above. The chiral separation of isomeric products contained in these samples was achieved on a 4.6×250 mm (5 μm) Chiralcel OJ-H column (Daicel, Chiral Technologies, Illkirch, France). An isocratic elution was performed with hexane/ethanol (70/30, v/v), using a flow rate of 0.5 ml/min and a detector absorbance wavelength of 214 nm. (+)-Catechin, (-)-catechin, and (-)-epicatechin were used as external standards. The retention time of (+)-epicatechin which was the only missing external standard was established from a previous study that included mass spectrometry and NMR investigations (Gargouri et al., 2009a).

LC/ESI-MS and -MS/MS of ANR reaction products

The regiospecificity of deuterium incorporation from pro(S)-NADPD into the final products was assessed by LC-MS and -MS/MS analysis. Non-deuterated catechins and epicatechins were used as external standards. The samples (20 μl) were separated using the Atlantis dc18 column (*vide infra*) connected to an electrospray ionization-ion trap mass spectrometer (Surveyor LC system and LCQ Advantage, Thermo Fisher, Waltham, MA, USA). The gradient was the same as that used for the routine HPLC assay, except that 0.05% formic acid was used instead of 0.08% trifluoroacetic acid. The 1-ml/min flow rate was split post-column, with a flow rate of only 0.2 ml/min being sent to the electrospray ionization source. The spectrometer was operated in the positive electrospray mode. The spray voltage was set to 4.5 kV, the capillary temperature was 270°C, and the capillary voltage was 32 V. MS/MS spectra of the major (M+1) parent ion derived from deuterated products, i.e., (epi)catechin or (epi)afzelechin, were obtained by means of collision-induced dissociation in the ion trap, using a normalized collision energy set at 35% of the instrument scale (Aimé et al., 2008).

Acknowledgments

We thank Dr. Bernard Badet (CNRS, UPR 2301, Gif-sur-Yvette, France) for helpful discussions.

References

Abrahams, S., Lee, E., Walker, A.R., Tanner, G.J., Larkin, P.J., and Ashton, A.R. (2003). The *Arabidopsis* TDS4 gene encodes leucoanthocyanidin dioxygenase (LDOX) and is essential for proanthocyanidin synthesis and vacuole development. Plant J. *35*, 624–636.

Aimé, C., Plet, B., Manet, S., Schmitter, J.M., Huc, I., Oda, R., Sauers, R.R., and Romsted, L.S. (2008). Competing gas-phase substitution and elimination reactions of gemini surfactants with anionic counterions by mass spectrometry. Density functional theory correlations with their bolaform halide salt models. J. Phys. Chem. B *112*, 14435–14445.

Gargouri, M., Manigand, C., Maugé, C., Granier, T., Langlois d'Estaintot, B., Cala, O., Piannet, I., Batany, K., Chaudière, J., and Gallois, B. (2009a). Structural and functional characterization of anthocyanidin reductase from *Vitis vinifera*. Acta Cryst. D *65*, 989–1000.

Gargouri, M., Gallois, B., and Chaudière, J. (2009b). Binding-equilibrium and kinetic studies of anthocyanidin reductase from *Vitis vinifera*. Arch. Biochem. Biophys. *491*, 61–68.

Gourley, D.G., Schüttelkopf, A.W., Leonard, G.A., Luba, J., Hardy, L.W., Beverley, S.M., and Hunter, W.N. (2001). Pteridine reductase mechanism correlates pterin metabolism with drug resistance in trypanosomatid parasites. Nat. Struct. Biol. *8*, 521–525.

Li, H.J. and Deinzer, M.L. (2007). Tandem mass spectrometry for sequencing proanthocyanidins. Anal. Chem. *79*, 1739–1748.

Louie, G.V., Baiga, T.J., Bowman, M.E., Koeduka, T., Taylor, J.H., Spassova, S.M., Pichersky, E., and Noel, J.P. (2007). Structure and reaction mechanism of basil eugenol synthase. PLoS One *2*, e993.

Petit, P., Granier, T., d'Estaintot, B.L., Manigand, C., Bathany, K., Schmitter, J.M., Lauvergeat, V., Hamdi, S., and Gallois, B. (2007). Crystal structure of grape dihydroflavonol 4-reductase, a key enzyme in flavonoid biosynthesis. J. Mol. Biol. *368*, 1345–1357.

Pfeiffer, J., Kühnel, C., Brandt, J., Duy, D., Punyasiri, P.A., Forkmann, G., and Fischer, T.C. (2006). Biosynthesis of flavan 3-ols by leucoanthocyanidin 4-reductases and anthocyanidin reductases in leaves of grape (*Vitis vinifera L.*), apple (*Malus× domestica Borkh.*) and other crops. Plant Physiol. Biochem. *44*, 323–334.

Saito, K., Kobayashi, M., Gong, Z., Tanaka, Y., and Yamazaki, M. (1999). Direct evidence for anthocyanidin synthase as a 2-oxoglutarate-dependent oxygenase: molecular cloning and functional expression of cDNA from a red forma of *Perilla frutescens*. Plant J. *17*, 181–189.

Shao, H., Dixon, R.A., and Wang, X. (2007). Crystal structure of vestitone reductase from alfalfa (*Medicago sativa* L.). J. Mol. Biol. *369*, 265–276.

Springob, K., Nakajima, J., Yamazaki, M., and Saito, K. (2003). Recent advances in the biosynthesis and accumulation of anthocyanins. Nat. Prod. Rep. *20*, 288–303.

Tanner, G.J., Francki, K.T., Abrahams, S., Watson, J.M., Larkin, P.J., and Ashton, A.R. (2003). Proanthocyanidin biosynthesis in plants. Purification of legume leucoanthocyanidin reductase and molecular cloning of its cDNA. J. Biol. Chem. *278*, 31647–31656.

Turnbull, J.J., Prescott, A.G., Schofield, C.J., and Wilmouth, R.C. (2001). Purification, crystallization and preliminary X-ray diffraction of anthocyanidin synthase from *Arabidopsis thaliana*. Acta Crystallogr. D Biol. Crystallogr. *57*, 425–427.

Veitch, N.C. and Grayer, R.J. (2008). Flavonoids and their glycosides, including anthocyanins. Nat. Prod. Rep. *25*, 555–611.

Wang, J., Leblanc, E., Chang, C.F., Papadopoulou, B., Bray, T., Whiteley, J.M., Lin, S.X., and Ouellette, M. (1997). Pterin and folate reduction by the *Leishmania tarentolae* H locus short-chain dehydrogenase/reductase PTR1. Arch. Biochem. Biophys. *342*, 197–202.

Wilmouth, R.C., Turnbull, J.J., Welford, R.W., Clifton, I.J., Prescott, A.G., and Schofield, C.J. (2002). Structure and mechanism of anthocyanidin synthase from *Arabidopsis thaliana*. Structure *10*, 93–103.

Wu, X., Liu, N., He, Y., and Chen, Y. (2009). Cloning, expression, and characterization of a novel diketoreductase from *Acinetobacter baylyi*. Acta Biochim. Biophys. Sin. (Shanghai) *41*, 163–170.

Xie, D.Y., Sharma, S.B., Paiva, N.L., Ferreira, D., and Dixon, R.A. (2003). Role of anthocyanidin reductase, encoded by BANYULS in plant flavonoid biosynthesis. Science *299*, 396–399.

Xie, D.Y., Sharma, S.B., and Dixon, R.A. (2004). Anthocyanidin reductases from *Medicago truncatula* and *Arabidopsis thaliana*. Arch. Biochem. Biophys. *422*, 91–102.

Received September 24, 2009; accepted October 29, 2009